

Production of $c\bar{c}c\bar{c}$ in double-parton scattering within k_t -factorization approach – meson-meson correlations

Rafał Maciuła*

Institute of Nuclear Physics PAN, PL-31-342 Cracow, Poland

Antoni Szczurek†

*Institute of Nuclear Physics PAN, PL-31-342 Cracow, Poland and
University of Rzeszów, PL-35-959 Rzeszów, Poland*

(Dated: March 6, 2018)

Abstract

We discuss production of two pairs of $c\bar{c}$ in proton-proton collisions at the LHC. Both double-parton scattering (DPS) and single-parton scattering (SPS) contributions are included in the analysis. Each step of DPS is calculated within k_t -factorization approach, i.e. effectively including next-to-leading order corrections. The conditions how to identify the DPS contribution are presented. The discussed mechanism unavoidably leads to the production of pairs of mesons: $D_i D_j$ (each containing c quarks) or $\bar{D}_i \bar{D}_j$ (each containing \bar{c} antiquarks). We calculate corresponding production rates for different combinations of charmed mesons as well as some differential distribution for $(D^0 D^0 + \bar{D}^0 \bar{D}^0)$ production. Within large theoretical uncertainties the predicted DPS cross section is fairly similar to the cross section measured recently by the LHCb collaboration. The best description is obtained with the Kimber-Martin-Ryskin (KMR) unintegrated gluon distribution, which very well simulates higher-order corrections. The contribution of SPS, calculated in the high-energy approximation, turned out to be rather small. Finally, we emphasize significant contribution of DPS mechanism to inclusive charmed meson spectra measured recently by ALICE, ATLAS and LHCb.

PACS numbers: 13.87.Ce,14.65.Dw

*Electronic address: rafal.maciula@ifj.edu.pl

†Electronic address: antoni.szczurek@ifj.edu.pl

I. INTRODUCTION

There has been recently renewed interest in studying double-parton scattering (DPS) effects in different reactions (see e.g. [1] and references therein). Very recently we have shown that the production of $c\bar{c}c\bar{c}$ is a very good place to study DPS effects [2]. Here, the quark mass is small enough to assure that the cross section for DPS is very large, and large enough that each of the scatterings can be treated within pQCD. The calculation performed in Ref. [2] were done in the leading-order (LO) collinear approximation. This may not be sufficient when comparing the results of the calculation with real experimental data. In the meantime the LHCb collaboration presented new interesting data for simultaneous production of two charmed mesons [3]. They have observed large percentage of the events with two mesons, both containing c quark, with respect to the typical production of the corresponding meson/antimeson pair ($\sigma_{D_i D_j} / \sigma_{D_i \bar{D}_j} \sim 10\%$), despite of the very limited LHCb acceptance.

Is the large effect a footprint of double parton scattering? We wish to address the issue in this paper. In addition, we shall estimate $c\bar{c}c\bar{c}$ production via single-parton scattering (SPS) within a high-energy approximation [4]. This approach should be an efficient tool especially when the distance in rapidity between cc or/and $c\bar{c}$ is large.

Another evidence for the DPS effects can be a missing cross section in the inclusive charmed meson distributions observed recently in Ref. [5]. The measured inclusive cross sections include events where two D (or two \bar{D}) mesons are produced, therefore corresponding theoretical predictions should also be corrected for the DPS effects.

In Ref. [6] the authors estimated DPS contribution based on the experimental inclusive D meson spectra measured at LHC which, as discussed in our paper, may be too crude approximation. In addition, in their approach fragmentation was included only in terms of the branching fractions for the transition $c \rightarrow D$. In our approach we shall include full kinematics of hadronization process. Here we wish to show also first differential distributions on the hadron level to be confronted with recent LHCb experimental data [3].

II. THEORETICAL FRAMEWORK

In the present analysis, when considering $pp \rightarrow c\bar{c}c\bar{c}X$ reaction, we concentrate primarily on double-parton scattering effects. In Section III.B we will show that the single-scattering contribution to double-charm production is much smaller, especially in the LHCb kinematics.

A. Double-parton scattering

In LO collinear approximation the differential distributions for $c\bar{c}$ production depend e.g. on rapidity of quark, rapidity of antiquark and transverse momentum of one of them (they are identical) [2]. In the next-to-leading order (NLO) collinear approach or in the k_t -factorization approach the situation is more complicated as there are more kinematical variables necessary to describe the kinematical situation. In the k_t -factorization approach the differential cross section for DPS production of $c\bar{c}c\bar{c}$ system, assuming factorization of

the DPS model, can be written as:

$$\frac{d\sigma^{DPS}(pp \rightarrow c\bar{c}c\bar{c}X)}{dy_1 dy_2 d^2 p_{1,t} d^2 p_{2,t} dy_3 dy_4 d^2 p_{3,t} d^2 p_{4,t}} = \frac{1}{2\sigma_{eff}} \cdot \frac{d\sigma^{SPS}(pp \rightarrow c\bar{c}X_1)}{dy_1 dy_2 d^2 p_{1,t} d^2 p_{2,t}} \cdot \frac{d\sigma^{SPS}(pp \rightarrow c\bar{c}X_2)}{dy_3 dy_4 d^2 p_{3,t} d^2 p_{4,t}}. \quad (2.1)$$

When integrating over kinematical variables one obtains

$$\sigma^{DPS}(pp \rightarrow c\bar{c}c\bar{c}X) = \frac{1}{2\sigma_{eff}} \sigma^{SPS}(pp \rightarrow c\bar{c}X_1) \cdot \sigma^{SPS}(pp \rightarrow c\bar{c}X_2). \quad (2.2)$$

These formulae assume that the two parton subprocesses are not correlated one with each other. The parameter σ_{eff} in the denominator of above formulae can be defined as:

$$\sigma_{eff} = \left[\int d^2 b (T(\vec{b}))^2 \right]^{-1}, \quad (2.3)$$

where the overlap function

$$T(\vec{b}) = \int f(\vec{b}_1) f(\vec{b}_1 - \vec{b}) d^2 b_1, \quad (2.4)$$

if the impact-parameter dependent double-parton distributions (dPDFs) are written in the following factorized approximation [7, 8]:

$$\Gamma_{i,j}(x_1, x_2; \vec{b}_1, \vec{b}_2; \mu_1^2, \mu_2^2) = F_{i,j}(x_1, x_2; \mu_1^2, \mu_2^2) f(\vec{b}_1) f(\vec{b}_2). \quad (2.5)$$

Experimental data from Tevatron [9] provide an estimate of σ_{eff} in the denominator of formula (2.2). Corresponding evaluations from the LHC are expected soon. In our analysis we take $\sigma_{eff} = 15$ mb. In the most general case one may expect some violation of this simple factorized Ansatz given by Eq. 2.2 [8].

In our present analysis cross section for each step is calculated in the k_t -factorization approach, that is:

$$\begin{aligned} \frac{d\sigma^{SPS}(pp \rightarrow c\bar{c}X_1)}{dy_1 dy_2 d^2 p_{1,t} d^2 p_{2,t}} &= \frac{1}{16\pi^2 \hat{s}^2} \int \frac{d^2 k_{1t}}{\pi} \frac{d^2 k_{2t}}{\pi} \overline{|\mathcal{M}_{g^*g^* \rightarrow c\bar{c}}|^2} \\ &\times \delta^2(\vec{k}_{1t} + \vec{k}_{2t} - \vec{p}_{1t} - \vec{p}_{2t}) \mathcal{F}(x_1, k_{1t}^2, \mu^2) \mathcal{F}(x_2, k_{2t}^2, \mu^2), \\ \frac{d\sigma^{SPS}(pp \rightarrow c\bar{c}X_2)}{dy_3 dy_4 d^2 p_{3,t} d^2 p_{4,t}} &= \frac{1}{16\pi^2 \hat{s}^2} \int \frac{d^2 k_{3t}}{\pi} \frac{d^2 k_{4t}}{\pi} \overline{|\mathcal{M}_{g^*g^* \rightarrow c\bar{c}}|^2} \\ &\times \delta^2(\vec{k}_{3t} + \vec{k}_{4t} - \vec{p}_{3t} - \vec{p}_{4t}) \mathcal{F}(x_3, k_{3t}^2, \mu^2) \mathcal{F}(x_4, k_{4t}^2, \mu^2). \end{aligned} \quad (2.6)$$

The matrix elements for $g^*g^* \rightarrow c\bar{c}$ (off-shell gluons) must be calculated including transverse momenta of initial gluons as it was done first in [10–12]. The unintegrated (k_t -dependent) gluon distributions (UGDFs) in the proton are taken from the literature [13–15]. Due to the emission of soft gluons encoded in these objects, it is believed that a major part of NLO corrections is effectively included. This is in analogy to initial state parton shower in Monte Carlo generators and strongly depends on technical construction of UGDF (see Ref. [5]). The framework of the k_t -factorization approach is often used with success in describing inclusive spectra of D or B mesons as well as for theoretical predictions for so-called nonphotonic leptons, products of semileptonic decays of charm and bottom mesons [16–22].

B. Single-parton scattering

The total cross section for the production of $c\bar{c}c\bar{c}$ final state via single gluon-gluon interaction can be calculated in the parton model approach as:

$$\sigma(pp \rightarrow c\bar{c}c\bar{c}; W^2) = \int dx_1 dx_2 g(x_1, \mu_F^2) g(x_2, \mu_F^2) \sigma(gg \rightarrow c\bar{c}c\bar{c}; x_1 x_2 W^2). \quad (2.7)$$

Here $g(x, \mu^2)$ is integrated (collinear) gluon distribution in a proton (PDF), and W is the proton-proton center of mass energy. In practice the integration is done in $\log_{10} x_1$ and $\log_{10} x_2$, including the corresponding jacobian of transformation. The elementary cross section of Eq. (2.7) enters at $\hat{s} = x_1 x_2 W^2 > 16m_c^2$. The parton level cross section in (2.7) is therefore very useful in order to obtain differential distributions in invariant mass of the $c\bar{c}c\bar{c}$ system.

In the present calculation we concentrate on LHC energies and consider the $gg \rightarrow c\bar{c}c\bar{c}$ subprocesses only. In the high-energy approximation the elementary cross section can be written in the compact form (see Ref. [4]):

$$d\sigma(gg \rightarrow c\bar{c}c\bar{c}) = \frac{N_c^2 - 1}{N_c^2} \frac{4\pi^2 \alpha_s^2}{[\vec{q}^2 + \mu_G^2]^2} I_{g \rightarrow c\bar{c}}(z_1, \vec{k}_1, \vec{q}) I_{g \rightarrow c\bar{c}}(z_2, \vec{k}_2, -\vec{q}) dz_1 \frac{d^2 k_1}{(2\pi)^2} dz_2 \frac{d^2 k_2}{(2\pi)^2} \frac{d^2 q}{(2\pi)^2}. \quad (2.8)$$

Here the $I_{g \rightarrow c\bar{c}}(z_1, \vec{k}_1, \vec{q}_1)$ and $I_{g \rightarrow c\bar{c}}(z_2, \vec{k}_2, \vec{q}_2)$ factors, called impact factors, describe the coupling of pairs of $c\bar{c}$ associated with the first and second gluon/proton, respectively. Above z_1 and z_2 are longitudinal momentum fractions of quarks with respect to parent gluons in the first and second pair, respectively, and \vec{k}_i their respective transverse momenta, \vec{q} is exchanged transverse momentum and μ_G is gluon mass which can be put to zero at least mathematically. At low energies this formula must be corrected for threshold effects [4]. The differential cross sections for $pp \rightarrow c\bar{c}c\bar{c}X$ can be obtained by replacing the $\sigma(gg \rightarrow c\bar{c}c\bar{c})$ by $d\sigma(gg \rightarrow c\bar{c}c\bar{c})$ in Eq.(2.7). Details about how the arguments of α_s are chosen are discussed in Ref. [4].

Our approach includes subprocesses coherently to be contrasted to Ref. [6] where they were separated one from each other to simplify calculations. In addition, we get a practical agreement with results of calculations in Ref. [23].

C. Double meson production

Kinematical correlations between quarks and antiquarks are not accessible experimentally. Instead one can measure correlations between heavy mesons or nonphotonic electrons. In this paper we will analyze kinematical correlations between charmed mesons. In particular, we are interested in correlations between D_i and D_j mesons (both containing c quark) or between \bar{D}_i and \bar{D}_j mesons (both containing \bar{c} antiquark). In order to calculate correlations between mesons we follow here the fragmentation function technique for hadronization process:

$$\frac{d\sigma(pp \rightarrow DDX)}{dy_1 dy_2 d^2 p_{1,t}^D d^2 p_{2,t}^D} \approx \int \frac{D_{c \rightarrow D}(z_1)}{z_1} \cdot \frac{D_{c \rightarrow D}(z_2)}{z_2} \cdot \frac{d\sigma(pp \rightarrow ccX)}{dy_1 dy_2 d^2 p_{1,t}^c d^2 p_{2,t}^c} dz_1 dz_2, \quad (2.9)$$

where: $p_{1,t}^c = \frac{p_{1,t}^D}{z_1}$, $p_{2,t}^c = \frac{p_{2,t}^D}{z_2}$ and meson longitudinal fractions $z_1, z_2 \in (0, 1)$. We have made approximation assuming that y_1, y_2 and ϕ are unchanged in the fragmentation process. The multidimensional distribution for both c quarks (or both \bar{c} antiquarks) is convoluted with fragmentation functions simultaneously for each of the two quarks (or each of the two antiquarks). As a result of the hadronization one obtains corresponding two-meson multidimensional distribution. In the last step experimental kinematical cuts on the distributions can be imposed. Then the resulting distributions can be compared with experimental ones. For numerical calculations here we apply often used in the case of heavy quarks, the Peterson fragmentation function [24]. We have shown in Ref. [5] that this scheme works very well in the case of inclusive D^0 meson spectra as well as for $D^0\bar{D}^0$ kinematical correlations.

III. RESULTS

A. Parton level

We start from inclusive distributions of charm quarks (or antiquarks). As discussed in Ref. [5] the standard single-parton scattering contribution to $pp \rightarrow c\bar{c}X$ seems insufficient to describe inclusive spectra of charmed mesons as measured by the ATLAS, ALICE and LHCb collaborations [25–27]. The $c\bar{c}c\bar{c}$ production also contributes to the inclusive charm production. In Fig. 1 we show such a contribution to transverse momentum distribution (left panel) and rapidity distribution (right panel) together with theoretical uncertainty band. In this calculation the Kimber-Martin-Ryskin (KMR) UGDF [13] was used with the MSTW08 [28] collinear gluon PDF. The solid line corresponds to central value of our predictions. The uncertainties are obtained by changing charm quark mass $m_c = 1.5 \pm 0.3$ GeV which in general is not well known and by varying renormalization and factorization scales $\mu^2 = \mu_R^2 = \mu_F^2 = \zeta m_t^2$, where $\zeta \in (0.5; 2)$. The shaded bands represent these both sources of uncertainties summed in quadrature. As a reference point we plot contribution from standard single-scattering $c\bar{c}$ production, obtained in the k_t -factorization approach (long-dashed line) as well as calculated with the help of FONLL code [29] (dash-dotted line). As can be seen both of these models are consistent and give very similar numerical results. It suggests that in the case of charm quark production the k_t -factorization approach with the KMR UGDFs very well reproduces NLO corrections. These aspects of $c\bar{c}$ production were discussed in more detail in Ref. [5].

Since the DPS uncertainty band is very broad it becomes clear that this contribution is quite sizeable and must be included in the total balance of charm quark (antiquark) production. For comparison we show also DPS result obtained previously in Ref. [2] in the LO collinear approach. It is much smaller than the k_t -factorization result, especially at larger transverse momenta.

In Fig. 2 we compare DPS results for transverse momentum (left panel) and rapidity (right panel) distributions obtained with different UGDFs from the literature [13–15]. The KMR UGDF gives the largest cross section. Numerical results of DPS are more sensitive to the choice of UGDFs than in the case of SPS $c\bar{c}$ production, which can be understood by different power of UGDFs in the cross section formula (fourth in DPS $c\bar{c}c\bar{c}$ versus second in SPS $c\bar{c}$). We use here also the KMS [14] and Jung setA+ [15] parametrizations. In turn, in Fig. 3 we confront theoretical uncertainties of SPS single pair ($c\bar{c}$) and DPS two-pair ($c\bar{c}c\bar{c}$) production. Again uncertainty of the two pair production is much larger than that for single

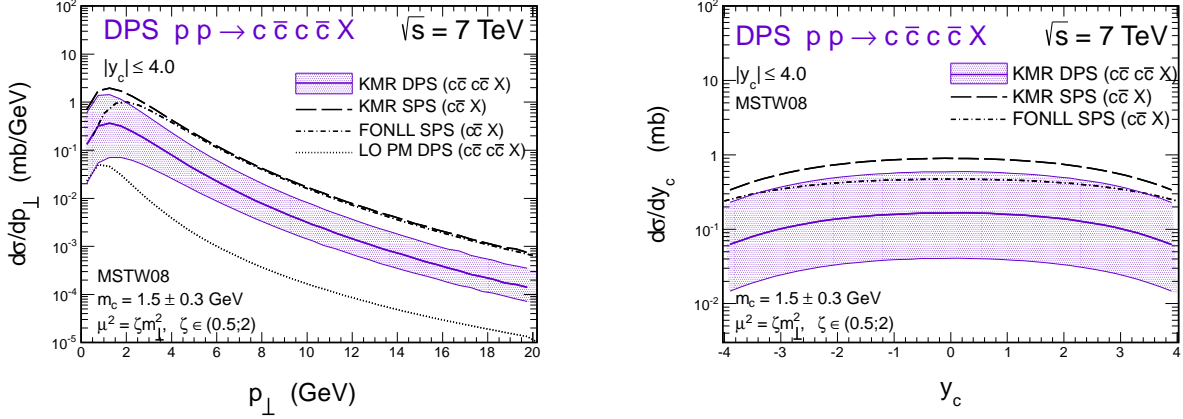


FIG. 1: Transverse momentum (left) and rapidity (right) of charm quarks from SPS $c\bar{c}$ (long-dashed line) and DPS $c\bar{c}c\bar{c}$ (solid line with shaded band) production. In this calculation the KMR UGDF was used and the factorization scale and quark mass for the DPS contribution were varied as explained in the figure. For comparison LO collinear DPS distribution (dotted line) and FONLL SPS $c\bar{c}$ result (dash-dotted line) are shown.

pair production.

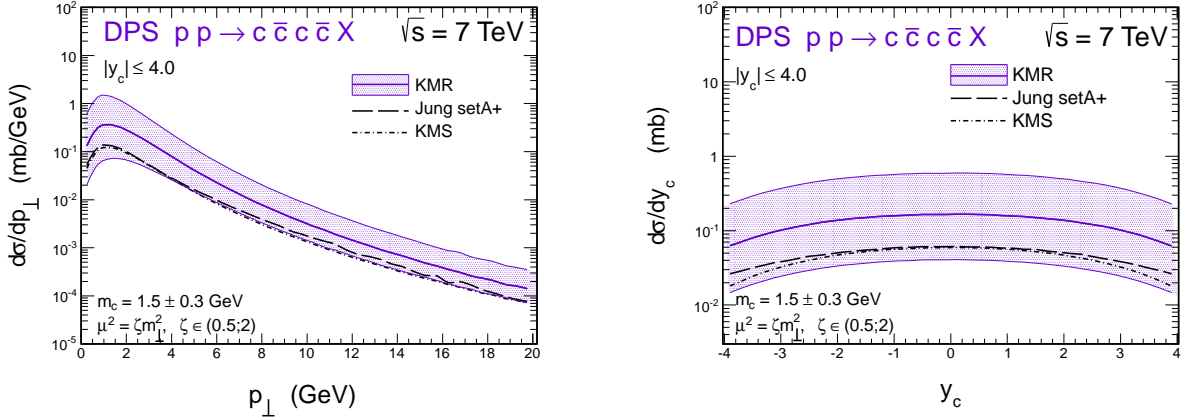


FIG. 2: Transverse momentum (left) and rapidity (right) distributions of charm quarks produced in DPS $c\bar{c}c\bar{c}$ production for different unintegrated gluon distributions.

In Ref. [2] we have proposed several correlation distributions to be studied in order to identify the DPS effects. Here we present the same distributions as in Ref. [2] but within the k_t -factorization approach. In Fig. 4 we show distributions in invariant mass $M_{c\bar{c}}$ (left panel) and rapidity difference of quarks/antiquarks $Y_{diff} = y_c - y_{\bar{c}}$ (right panel) from the same scattering ($c_1\bar{c}_2$ or $c_3\bar{c}_4$) and from different scatterings ($c_1\bar{c}_4$ or $c_3\bar{c}_2$ or c_1c_3 or $\bar{c}_2\bar{c}_4$) for various UGDFs specified in the figure. The shapes of distributions in the figure are almost identical as their counterparts obtained in LO collinear approach in Ref. [2].

In Fig. 5 we show distributions in azimuthal angle difference between quarks/antiquarks $\varphi_{c\bar{c}}$ from the same and from different scatterings. While in the case of the same scattering distribution strongly depends on the choice of UGDF the quarks/antiquarks from different scattering are not correlated which is inherent property of the simple factorized model. Our

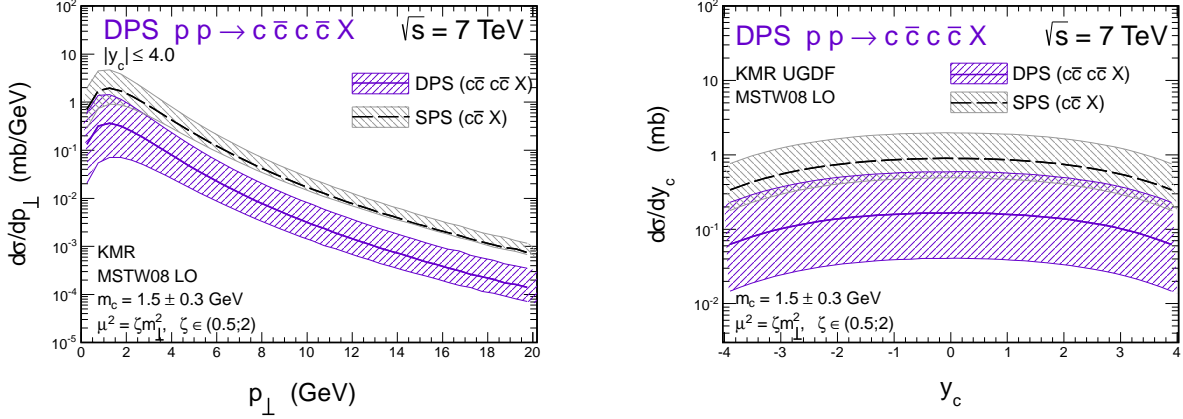


FIG. 3: Comparison of the SPS $c\bar{c}$ and DPS $c\bar{c}c\bar{c}$ contributions to the inclusive charm quark (antiquark) production together with theoretical uncertainties due to the choice of scales and those related with quark mass (summed in quadrature).

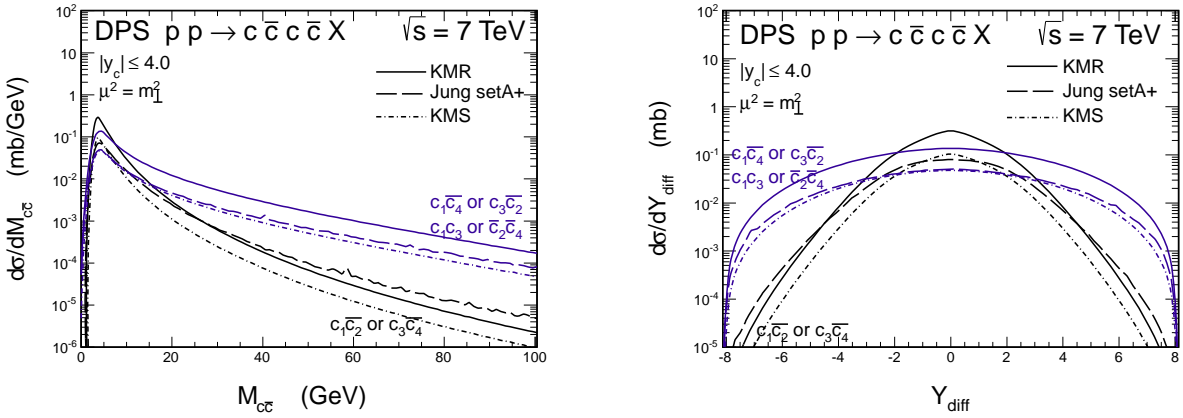


FIG. 4: Distribution in the invariant mass of quark/antiquark $M_{c\bar{c}}$ (left) and distribution in the rapidity distance between quarks/antiquarks Y_{diff} (right) from the same ($c_1\bar{c}_2$ or $c_3\bar{c}_4$) and from different scatterings ($c_1\bar{c}_4$ or $c_3\bar{c}_2$ or c_1c_3 or $\bar{c}_2\bar{c}_4$), calculated with different UGDFs.

distinguishing of scatterings can be done only in the model calculation. Experimentally one observes both types together after hadronization which naturally may bring additional decorrelation.

Finally, we present distribution in transverse momentum of the pair of quarks $p_{\perp}^{c\bar{c}}$. In LO collinear approach the distribution for emission in the same scattering is very different from the case of emissions from different scatterings [2]. The picture in the k_t -factorization approach is, however, very different. The respective distributions for the same and different scatterings are rather similar. This means that transverse momentum of the pair may not be the best quantity to be used in order to identify the DPS effects.

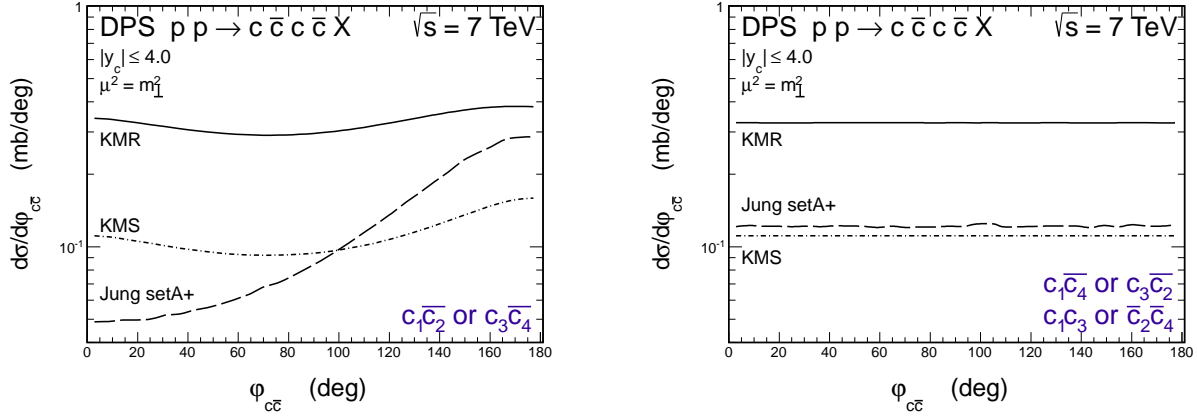


FIG. 5: Distribution in azimuthal angle $\varphi_{c\bar{c}}$ between quarks/antiquarks from the same scattering (left) and from different scatterings (right), calculated with different UGDs.

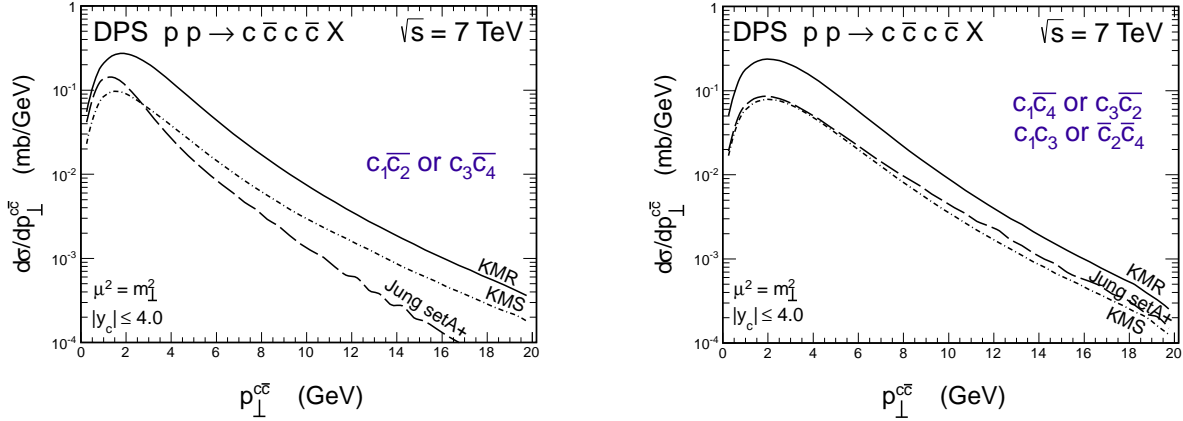


FIG. 6: Distribution in transverse momentum of the quark/antiquark pair $p_{\perp}^{c\bar{c}}$ from the same scattering (left) and from different scatterings (right), calculated with different UGDs.

B. Meson level

Production of two pairs of $c\bar{c}$ on the partonic level leads to the situations that very often two mesons, both containing c quarks or/and both containing \bar{c} antiquarks, are produced on the hadronic level in one event. Therefore the presence of two such mesons may be considered as a signal of production of $c\bar{c}c\bar{c}$ on the partonic level. Recently, the LHCb collaboration performed a first measurement of $D_i D_j + \bar{D}_i \bar{D}_j$ production in the fiducial range of the detector acceptance $2 < y_D < 4$ and $3 < p_{\perp}^D < 12$ GeV [3]. As described in Section II we have prepared a code which keeps track of full kinematical information about each of both quarks or both antiquarks and similar information about both mesons. Such a multidimensional map is used then to impose adequate experimental cuts.

In Table 1 we have collected DPS cross sections for different pairs of mesons relevant for considered kinematics obtained with different unintegrated gluon distributions. As was shown in Ref. [5] theoretical predictions for production of charmed meson pairs in the LHCb kinematics are very sensitive to the value of ε_c parameter in the Peterson fragmentation

TABLE I: Total cross sections for meson-meson pair production for three different UGDFs.

Mode	σ_{tot}^{EXP} [nb]	σ_{tot}^{THEORY} [nb]					
		KMR $^+(\mu)$ $^+(m_c)$		Jung setA+		KMS	
		$\varepsilon_c = 0.05$	$\varepsilon_c = 0.02$	$\varepsilon_c = 0.05$	$\varepsilon_c = 0.02$	$\varepsilon_c = 0.05$	$\varepsilon_c = 0.02$
$D^0 D^0$	$690 \pm 40 \pm 70$	$265^{+140}_{-77}^{+157}_{-94}$	400	120	175	84	126
$D^0 D^+$	$520 \pm 80 \pm 70$	$212^{+112}_{-62}^{+126}_{-75}$	319	96	140	67	100
$D^0 D_S^+$	$270 \pm 50 \pm 40$	$75^{+40}_{-22}^{+45}_{-27}$	113	34	50	24	36
$D^+ D^+$	$80 \pm 10 \pm 10$	$42^{+23}_{-13}^{+26}_{-15}$	64	19	28	13	20
$D^+ D_S^+$	$70 \pm 15 \pm 10$	$30^{+16}_{-9}^{+18}_{-11}$	45	14	20	10	14
$D_S^+ D_S^+$	—	$11^{+5}_{-3}^{+6}_{-4}$	16	5	7	3	5

function. There, rather harder functions (with smaller ε_c) are suggested for better description of experimental data, which is also in agreement with observations made in the FONLL framework [30, 31]. Therefore we present results for two different values of the ε_c parameter. Here we have added together cross sections for charge conjugated channels: $\sigma_{D_i D_j} + \sigma_{\bar{D}_i \bar{D}_j}$. The calculated cross sections are somewhat smaller than the experimental ones. Only the upper limit of our predictions with the Kimber-Martin-Ryskin UGDF and with $\varepsilon_c = 0.02$ in the Peterson fragmentation function gives results which are close to the experimental data, taken the uncertainties on the choice of the factorization/renormalization scale and on the charm quark mass.

So far we have considered only DPS contribution to $D_i D_j$ (or $\bar{D}_i \bar{D}_j$) production. In Fig. 7 we show in addition corresponding SPS contribution. The SPS contribution to the transverse momentum distribution (left panel) is more than two orders of magnitude smaller than the DPS one. For the rapidity distribution (right panel) the difference is only one order of magnitude. This effect is slightly unintuitive. However, it can be understood by a comparison of the two-dimensional distributions in rapidity of one and the second D meson for DPS and SPS production (see Fig. 8). In the case of DPS the two mesons are not correlated (in this plane), in contrast to the SPS mechanism, where they are strongly anticorrelated. When one meson is produced in forward rapidity region the second is preferentially produced in backward rapidity region, or vice versa. One can also conclude that in the case of $D_i D_j$ ($\bar{D}_i \bar{D}_j$) pair production, the specific LHCb kinematical range leads to a dumping of the SPS cross section. The requirement that both D mesons have to reach the detector makes the SPS contribution almost negligible. Quite different conclusions can be drawn in the case of inclusive D meson measurements.

In the present paper we have calculated SPS $c\bar{c}c\bar{c}$ contribution in the high-energy approximation which may not be the best approximation for the LHCb kinematics where the distance between both c or both \bar{c} is rather small. Therefore, to draw definite conclusions, future studies of the $pp \rightarrow c\bar{c}c\bar{c}X$ process are needed and they must include a complete set of diagrams for the SPS $c\bar{c}c\bar{c}$ mechanism. Furthermore, if the improved calculations of SPS mechanism will not provide somewhat better description of the total cross sections measured by LHCb, one has to look for other mechanisms which can contribute and fill predicted missing strength.

The LHCb collaboration presented also several differential distributions for the simultaneous production of two DD and $\bar{D}\bar{D}$ mesons. Here we consider only examples for $D^0 D^0$

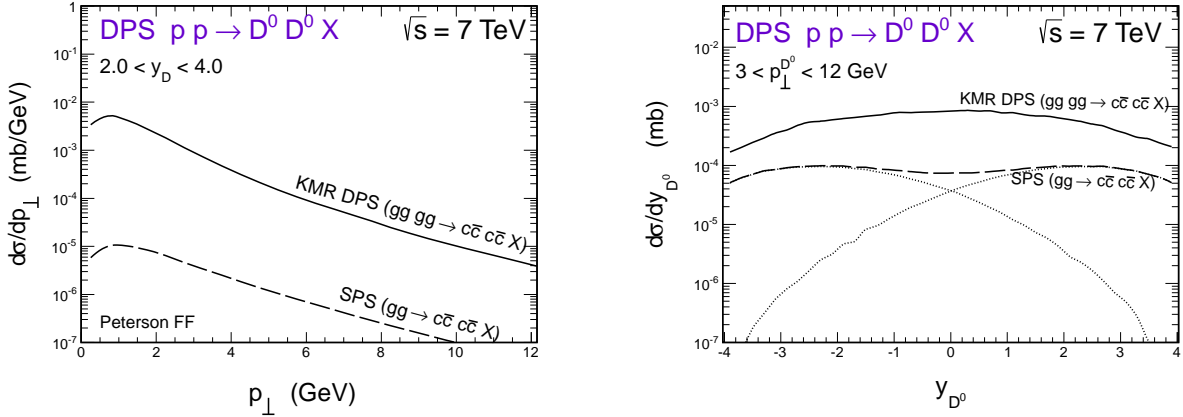


FIG. 7: Distributions in transverse momentum (left panel) and rapidity (right panel) of single D^0 meson from the D^0D^0 pair events. The solid lines correspond to DPS mechanism and the long-dashed lines represent contributions from SPS production of D^0D^0 pairs. Here we impose kinematical cuts adequate for the LHCb kinematics.

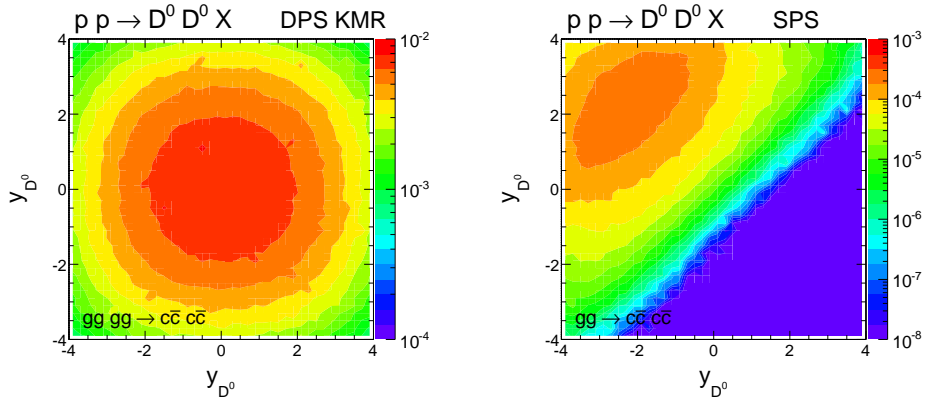


FIG. 8: Two-dimensional distributions in rapidity of one D^0 meson and rapidity of the second D^0 meson for DPS (left) and SPS (right).

(identical to $\bar{D}^0\bar{D}^0$) channel.

In Fig. 9 we present distribution in transverse momentum of one of the D^0 mesons, provided that both are measured within the LHCb experiment coverage specified in the figure caption. Our theoretical distributions have shapes in rough agreement with the experimental data. The shapes of the distributions are almost identical for different UGDFs used in the calculations (left panel) and are independent on the choice of scales in the case of the KMR model (right panel).

In Fig. 10 we show distribution in the D^0D^0 invariant mass $M_{D^0D^0}$ for both D^0 's measured in the kinematical region covered by the LHCb experiment. Here the shapes of the distributions have the same behavior for various UGDFs and are insensitive to changes of scales as in the previous figure. The characteristic minimum at small invariant masses is a consequence of experimental cuts (see Ref. [5]) and is rather well reproduced.

Finally in Fig. 11 we show distribution in azimuthal angle $\varphi_{D^0D^0}$ between both D^0 's. While the theoretical DPS contribution is independent of the relative azimuthal angle, there

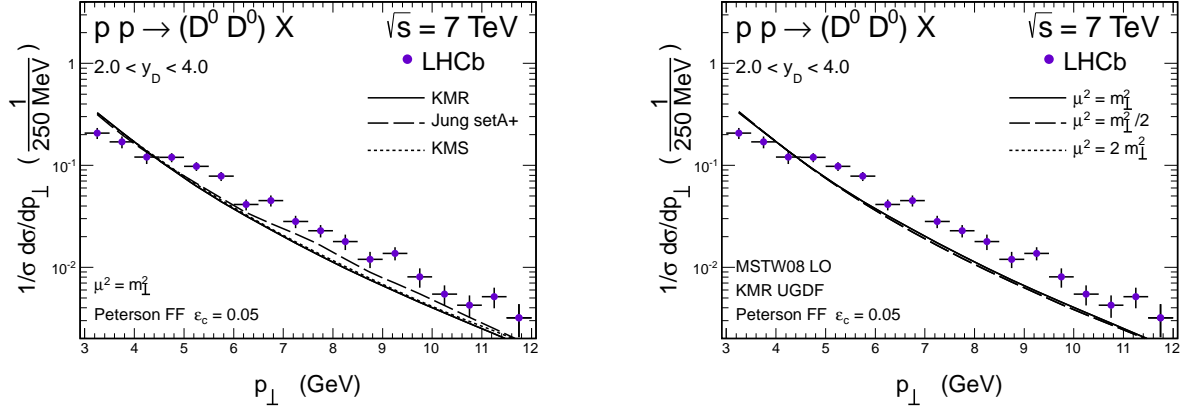


FIG. 9: Transverse momentum distribution of D^0 mesons from the $D^0 D^0$ pair contained in the LHCb kinematical region. The left panel shows dependence on UGDFs, while the right panel illustrates dependence of the result for the KMR UGDF on the factorization/renormalization scales.

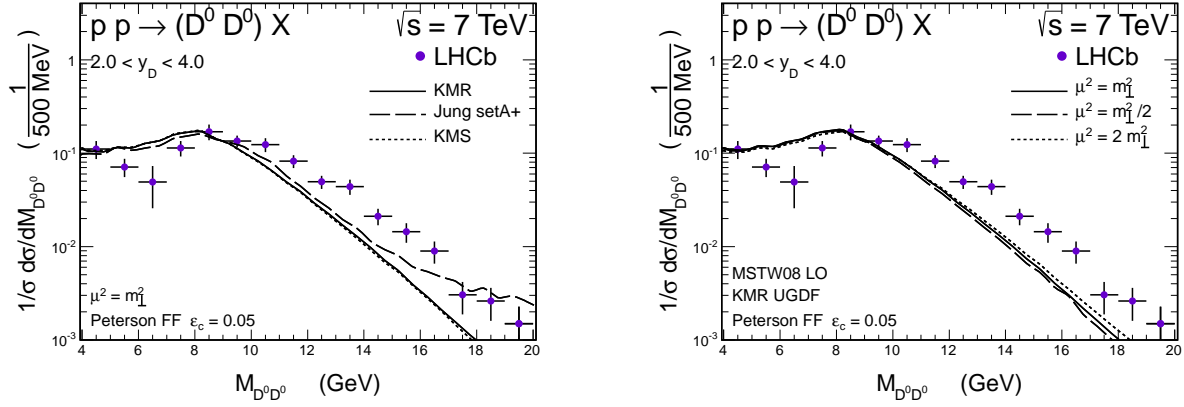


FIG. 10: $M_{D^0 D^0}$ invariant mass distribution for $D^0 D^0$ contained in the LHCb kinematical region. The left panel shows dependence on UGDFs, while the right panel illustrates dependence of the result for the KMR UGDF on the factorization/renormalization scales.

is some small residual dependence on azimuthal angle in experimental distribution. This may show that there is some missing mechanism which gives contributions both at small and large $\Delta\varphi$. However, this discrepancy may be also an inherent property of the DPS factorized model which does not allow for any azimuthal correlations between particles produced in different hard scatterings. We wish to emphasize in this context that the angular azimuthal correlation pattern for $D^0 \bar{D}^0$, discussed in Ref. [5], and for $D^0 D^0$ ($\bar{D}^0 \bar{D}^0$), discussed here, are quite different. The distribution for $D^0 D^0$ ($\bar{D}^0 \bar{D}^0$) is much more flat compared to the $D^0 \bar{D}^0$ one which shows a pronounced maximum at $\varphi_{D^0 \bar{D}^0} = 180^\circ$ (mostly from pair creation) and $\varphi_{D^0 \bar{D}^0} = 0^\circ$ (mostly from gluon splitting) [5]. This qualitative difference is in our opinion a model independent proof of the dominance of DPS effects in the production of $D^0 D^0$ ($\bar{D}^0 \bar{D}^0$).

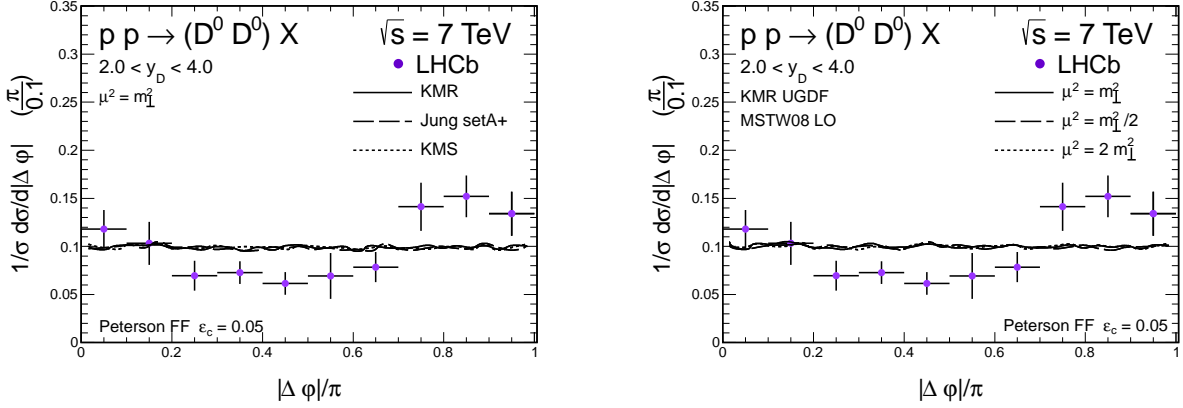


FIG. 11: Distribution in azimuthal angle $\varphi_{D^0 D^0}$ between both D^0 's. The left panel shows dependence on UGDFs, while the right panel illustrates dependence of the result for the KMR UGDF on the factorization/renormalization scales.

C. DPS $c\bar{c}c\bar{c}$ production and inclusive charmed meson distributions

Since the DPS cross section is very large it is also very important to look at the DPS $c\bar{c}c\bar{c}$ contribution to inclusive charmed meson spectra. Let us consider for example transverse momentum distribution of a charmed D_i meson. The corresponding DPS $c\bar{c}c\bar{c}$ contribution can be written as:

$$\begin{aligned}
\frac{d\sigma_{inc}^{D_i, DPS}}{dp_t} &= P_{D_i}(1 - P_{D_i}) \frac{d\sigma^D}{dp_{1,t}} \Big|_{p_{1,t}=p_t} (-2.1 < \eta_1 < 2.1, -\infty < \eta_2 < \infty) \\
&+ P_{D_i}(1 - P_{D_i}) \frac{d\sigma^D}{dp_{2,t}} \Big|_{p_{2,t}=p_t} (-\infty < \eta_1 < \infty, -2.1 < \eta_2 < 2.1) \\
&+ P_{D_i}P_{D_i} \frac{d\sigma^D}{dp_{1,t}} \Big|_{p_{1,t}=p_t} (-2.1 < \eta_1 < 2.1, -\infty < \eta_2 < \infty) \\
&+ P_{D_i}P_{D_i} \frac{d\sigma^D}{dp_{2,t}} \Big|_{p_{2,t}=p_t} (-\infty < \eta_1 < \infty, -2.1 < \eta_2 < 2.1). \quad (3.1)
\end{aligned}$$

In the formula above P_{D_i} is a shorthand notation for the branching fraction $P_{c \rightarrow D_i}$ and σ^D is the cross section for D -mesons assuming artificially the branching fraction equal to 1. The formula above can be somewhat simplified when combining similar terms.

In Fig. 12 we show inclusive one pair (long-dashed line), inclusive DPS two-pair contribution (dotted line) and the sum of both terms to transverse momentum distribution of different D mesons (solid line). The DPS $c\bar{c}c\bar{c}$ contribution is of the same order as the standard traditional SPS $c\bar{c}$ contribution. This is a completely new situation compared to what it was at smaller energies. The sum of both contributions almost describes the different experimental data. As discussed in the previous section the SPS $c\bar{c}c\bar{c}$ contribution can be of the order of 10% of the DPS $c\bar{c}c\bar{c}$ contribution. At higher energies one could expect even relatively larger DPS $c\bar{c}c\bar{c}$ contribution. A problem could start, however, that then one enters the region of really small gluon longitudinal momentum fractions $x < 10^{-4}$ for which

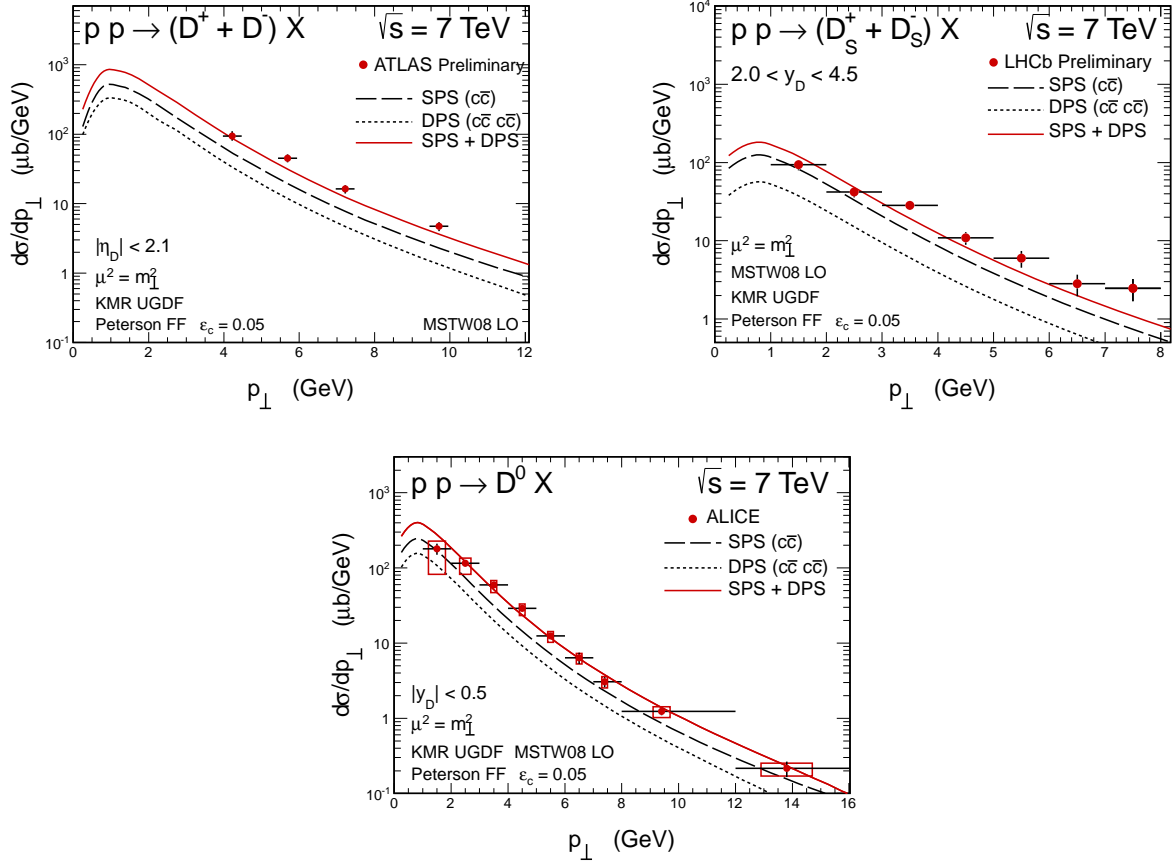


FIG. 12: Inclusive transverse momentum distributions of different charmed mesons measured by different groups at the LHC. The long-dashed line corresponds to the standard SPS $c\bar{c}$ production and the dotted line represents the DPS $c\bar{c}c\bar{c}$ contribution.

the gluon UGDFs (or PDFs) are not well known. In this case realistic models of UGDFs are badly needed. Do we have such a distribution at present?

IV. CONCLUSIONS

In this paper we have discussed production of $c\bar{c}c\bar{c}$ in the double-parton scattering (DPS) and single-parton scattering (SPS) in the $gg \rightarrow c\bar{c}c\bar{c}$ subprocess. The double-parton scattering is calculated in the factorized Ansatz with each step calculated in the k_t -factorization approach, i.e. including effectively higher-order QCD corrections.

The cross section in the k_t -factorization approach turned out to be much larger than its counterpart calculated in the LO collinear approach. The distribution in rapidity difference between quarks/antiquarks from the same and different scatterings turned out to have similar shape as in the LO collinear approach. The same is true for invariant masses of pairs of quark-quark, antiquark-antiquark and quark-antiquark, etc. The distribution in transverse momentum of the pair from the same scattering turned out to be similar to that for the pairs originating from different scatterings.

We have calculated also cross sections for the production of $D_i D_j$ (both containing c quark) and $\bar{D}_i \bar{D}_j$ (both containing \bar{c} antiquark) pairs of mesons. The results of the calculation have been compared to recent results of the LHCb collaboration.

The total rates of the meson pair production depend on the unintegrated gluon distributions. The best agreement with the LHCb result has been obtained for the Kimber-Martin-Ryskin UGDF. This approach as discussed already in the literature effectively includes higher-order QCD corrections.

As an example we have also calculated several differential distributions for $D^0 D^0$ pair production. Rather good agreement has been obtained for transverse momentum distribution of D^0 (\bar{D}^0) mesons and $D^0 D^0$ invariant mass distribution. The distribution in azimuthal angle between both D^0 's suggests that some contributions may be still missing. The single parton scattering contribution, calculated in the high energy approximation, turned out to be rather small. This should be checked in exact $2 \rightarrow 4$ parton model calculations in the future.

We have shown that the DPS mechanism of $c\bar{c}c\bar{c}$ production gives a new significant contribution to inclusive charmed meson spectra. For instance the description of the inclusive ATLAS, ALICE and LHCb data is very difficult in terms of the conventional SPS ($c\bar{c}$) contribution [5].

Since we have shown that the DPS mechanism gives significant contribution to inclusive spectra of charmed mesons the estimate of DPS effects, presented in Ref. [6] and based on experimental inclusive cross section, leads to an overestimation of the DPS effect.

Summarizing, the present study of $c\bar{c}c\bar{c}$ reaction in the k_t -factorization approach has shown that this reaction is an extremely good testing ground of double-parton scattering effects. The LHCb kinematics is not the best in this respect. Both ATLAS and CMS collaborations could measure the production of pairs of $D_i D_j$ and/or $\bar{D}_i \bar{D}_j$ mesons with large rapidity distance where the DPS mechanism is predicted to clearly dominate over the SPS mechanism. Another potentially interesting place to investigate DPS effect is the $pp \rightarrow J/\psi J/\psi X$ reaction [32]. Similarly as for $pp \rightarrow c\bar{c}c\bar{c}X$ discussed here, the large rapidity gap between two J/ψ 's should select clear sample of DPS mechanism.

Acknowledgments

The authors thank Ivan Belyaev and Marek Szczekowski for useful discussions of many aspects of the LHCb experimental data and Wolfgang Schäfer for discussion of single par-

ton scattering contribution. This work is supported in part by the Polish Grants DEC-2011/01/B/ST2/04535 and N202 237040.

- [1] P. Bartalini et al., arXiv:1111.0469 [hep-ph];
ANL-HEP-PR-11-65; CMS-CR-2011-048; DESY 11-185.
- [2] M. Luszczak, R. Maciuła and A. Szczurek, Phys. Rev. **D85** (2012) 094034.
- [3] R. Aaij et al. (The LHCb collaboration), J. High Energy Phys. **06** (2012) 141.
- [4] W. Schäfer and A. Szczurek, Phys. Rev. **D85** (2012) 094029.
- [5] R. Maciuła and A. Szczurek, arXiv:1301.3033 [hep-ph].
- [6] A.V. Berezhnoy et al., Phys. Rev. **D86** (2012) 034017.
- [7] J.R. Gaunt and W.J. Stirling, JHEP **1003** (2010) 005.
- [8] C. Flensburg, G. Gustafson, L. Lönnblad and A. Ster, J. High Energy Phys. **06** (2011) 066.
- [9] F. Abe et al. (CDF Collaboration), Phys. Rev. **D56** (1997) 3811;
Phys. Rev. Lett. **79** (1997) 584.
- [10] S. Catani, M. Ciafaloni and F. Hautmann, Nucl. Phys. **366** (1991) 135.
- [11] J.C. Collins and R.K. Ellis, Nucl. Phys. **B360** (1991) 3.
- [12] R.D. Ball and R.K. Ellis, J. High Energy Phys. **05** (2001) 053.
- [13] M.A. Kimber, A.D. Martin and M.G. Ryskin, Phys. Rev. **D63** (2001) 114027.
- [14] J. Kwieciński, A.D. Martin and A.M. Staśto, Phys. Rev. **D56** (1997) 3991.
- [15] H. Jung, G.P. Salam, Eur. Phys. J. **C19** (2001) 351;
H. Jung, arXiv:0411287 [hep-ph].
- [16] Ph. Högler, R. Kirschner, A. Schäfer, I. Szymanowski and O.V Teryaev,
Phys. Rev. **D62** (2000) 071502.
- [17] S.P. Baranov and M. Smizanska, Phys. Rev. **D62** (2000) 014012.
- [18] S.P. Baranov, A.V. Lipatov and N.P. Zotov, Phys. Atom. Nucl. **67** (2004) 837;
Yad. Fiz. **67** (2004) 856.
- [19] Yu.M. Shabelski and A.G. Shuvaev, Phys. Atom. Nucl. **69** (2006) 214.
- [20] M. Luszczak, R. Maciuła and A. Szczurek, Phys. Rev. **D79** (2009) 034009.
- [21] R. Maciuła, A. Szczurek and G. Ślipek, Phys. Rev. **D83** (2011) 054014.
- [22] H. Jung, M. Kraemer, A.V. Lipatov and N.P. Zotov, Phys. Rev. **D85** (2012) 034035;
J. High Energy Phys. **01** (2011) 085.
- [23] V.D. Barger, A.L. Stange and R.J.N. Phillips, Phys. Rev. **D44** (1991) 1987.
- [24] C. Peterson, D. Schlatter, I. Schmitt, P.M. Zerwas, Phys. Rev. **D27** (1983) 105.
- [25] The ATLAS collaboration, ATLAS-CONF-2011-017.
- [26] B. Abelev et al. (The ALICE collaboration), J. High Energy Phys. **01** (2012) 128.
- [27] The LHCb collaboration, LHCb-CONF-2010-013.
- [28] A.D. Martin, W.J. Stirling, R.S. Thorne and G. Watt, Eur. Phys. J. **C63** (2009) 189;
Eur. Phys. J. **C64** (2009) 653.
- [29] M. Cacciari, M. Greco and P. Nason, J. High Energy Phys. **05** (1998) 007;
M. Cacciari, S. Frixione and P. Nason, J. High Energy Phys. **03** (2001) 006.
- [30] M. Cacciari, P. Nason and R. Vogt, Phys. Rev. Lett. **95** (2005) 122001.
- [31] M. Cacciari et al., J. High Energy Phys. **10** (2012) 137.
- [32] S.P. Baranov, A.M. Snigirev, N.P. Zotov, A. Szczurek and W. Schäfer,
arXiv:1210.1806 [hep-ph].